Engenharia Agrícola

ISSN: 1809-4430 (on-line)

www.engenhariaagricola.org.br

Scientific Paper
Doi: http://dx.doi.org/10.1590/1809-4430-Eng.Agric.v44e20240063/2024

PARAMETER CALIBRATION OF RICE STRAW PARTICLE–CRUSHING MODEL

Shuying Jiang[1], DeZhi Ren[3], Fang Ma[1], Zhongyu Chen[1], Yanming Che[2*]

[2*]Corresponding author. Liaoning Agricultural Development Service Centre/Shenyang, China.
E-mail: 15950291869@163.com | ORCID ID: https://orcid.org/0009-0007-1096-3256

KEYWORDS

rice straw, Ab-T10 crushing model, parameter calibration, simulation, pulping.

ABSTRACT

Discrete element method is widely used to study grain particles; however, there is a lack of research on the mathematical model parameters of rice straw particles in the crushing simulation process. To determine suitable parameter settings for crushing of rice straw particles in the simulation process, a twin-screw rice straw crushing test device was built using rice straw particles as the research object. Through actual tests, the parameters of the Ab-T10 crushing models of rice straw particles with five different moisture contents were calibrated, and the crushing characteristics of the rice straw particles were analyzed. The Ab-T10 crushing models with calibrated parameters were verified by comparing the probability of the particle-size distribution (t_{10}) between the simulation and actual tests. The results show that the crushing probability and t_{10} of rice straw increase with the increase in accumulated contact specific energy and decrease with the increase in rice straw moisture content. The minimum value of the fitting parameter between the simulated and measured values is 0.9654, which indicates that the calibrated Ab-T10 crushing model can accurately simulate the rice straw particle-crushing process. This study provides a reference for the analysis of crushing in subsequent rice straw pulping.

INTRODUCTION

Rice straw pulping is a key process in pulp molding (Wang, 2022). The fibrillation of rice straw directly affects the quality of rice straw pulp. A twin-screw crushing device is typically used to fibrillate rice straw (Tian et al., 2023), such that the rice straw particles are subjected to various forces such as grinding, collision, and crushing in the rolling chamber to achieve the effect of grinding and crushing. Therefore, the grinding and crushing characteristics of rice straw particles are important for optimizing the structure and working parameters of twin-screw crushing devices.

Particle-crushing models include the bonded particle model (BPM), fast breakage model (FBM), and particle replacement model (PRM) (Zhang et al., 2022). Among them, FBM can simulate the particle-crushing process and particle-size distribution of broken particles (sub-particles) more accurately, making it suitable for simulating the material-crushing process. The Ab-T10 breakage model (belonging to the FBM) in the Rocky DEM software was used to simulate the material-crushing process (Shi et al., 2024a), where the sub-particles have a polyhedral shape, and the sub-particle-size distribution can be defined by the Gaudin–Schumann model (Camalan, 2020). When the Hertz–Mindlin with bonding model (belonging to BPM) in the EDEM software was adopted to simulate the material-crushing process during rolling (Lai et al., 2012), the sub-particles are spherical or spherical aggregates, which differ significantly from the actual shape of the sub-particles during crushing. Therefore, the Ab-T10 breakage model in the Rocky DEM software is more suitable for simulating the crushing process.

Parameter calibration of the crushing model is the foundation for accurately simulating the crushing process. The EDEM software was used to simulate uniaxial compression (or shear) crushing tests and establish regression equations between the key bonding parameters and the crushing force (Wu et al., 2024). Based on the actual crushing force, bonding parameters were determined during the calibration process and used to

[1] School of Yancheng Polytechnic College/Yancheng, China.
[2] Liaoning Agricultural Development Service Centre/Shenyang, China.
[3] School of Engineering College, Shenyang Agricultural University/Shenyang, China.

Area Editor: Gizele Ingrid Gadotti
Received in: 4-10-2024
Accepted in: 7-12-2024

calibrate the crushing model. The accuracy of the calibrated parameters was verified by comparing the measured and simulated values during the verification process. This parameter calibration method is not applicable to the Ab-T10 crushing model because of the difference between the principles of the Ab-T10 and the Hertz–Mindlin crushing models. Therefore, it is necessary to develop a parameter calibration method suitable for the Ab-T10 crushing model.

The Ab-T10 crushing model is only suitable for simulating the crushing of convex-shaped particles. However, rice straw particles are geometrically complex and are curved by quasi-surface particles. To improve the simulation accuracy of crushing process of the rice straw particles, it is necessary to complete the particle model. The conventional modeling approach for agricultural material particles approximates the particles as regular bodies, which is suitable for simple structures. Another modeling approach uses 3D laser scanning (Bi et al., 2021) or electronic computer tomography scanning (Chen et al., 2019) to obtain the profile of rice straw particles and build a particle model through particle filling. Although this can improve the accuracy of particle model construction, it still maintains the characteristics of irregular quasi-surface structures for modeling rice straw and other agricultural material particles and is not suitable for modeling convex particles (Singh et al., 2017). Therefore, it is necessary to explore a particle model construction method suitable for the Ab-T10 crushing model before simulating the crushing process of rice straw particles.

To explore the crushing characteristics of rice straw particles and calibrate the parameters of the Ab-T10 crushing model, a twin-screw crushing device was constructed in this study to measure the crushing probability and t_{10} of rice straw particles with five different moisture contents (Habert et al., 2020; Goda & Girardot, 2021). The parameters of the Ab-T10 crushing model were calibrated based on the test results. Using three-dimensional laser scanning technology, a rice straw particle model was built to simulate the crushing process of rice straw particles in a twin-screw crushing device based on the calibration results. The accuracy of the parameter calibration and particle model was verified by comparing t_{10} measured by simulations and test.

MATERIAL AND METHODS

Test Materials

Rice straw pretreated using a biomechanical method (Shahrubudin et al., 2019; Zhang et al., 2023) was used as the test material. Raw materials with a moisture content of 10% were used (Yu et al., 2020), based on the requirements of the “Clean Production Standard for the Paper Industry” (HJ/T 340-2007). Test samples with different moisture contents were prepared using biological agents and drying methods; the moisture contents of the test sample were 50.00%±2.50%, 55.00%±2.50%, 60.00%±2.50%, 65.00%±2.50%, and 70.00%±2.50%.

Test device

The characteristics of rice straw crushing and milling were investigated using a twin-screw crushing test device (Figure 1). The device comprises a crushing mechanism, electric motor, material feeding mechanism, and discharge mechanism. During the test, preprocessed rice straw was fed into the material feeding mechanism through the inlet. Feeding was kept uniform and appropriate to avoid blocking the apparatus. The material first entered the crushing mechanism through the feeding mechanism and was then crushed, collided, and pulverized by the twin-screw crushing mechanism before being sent to the discharge mechanism. The completely crushed slurry was collected using the discharge mechanism, and the particle-crushing probability and t_{10} were analyzed by opening the discharge mechanism.

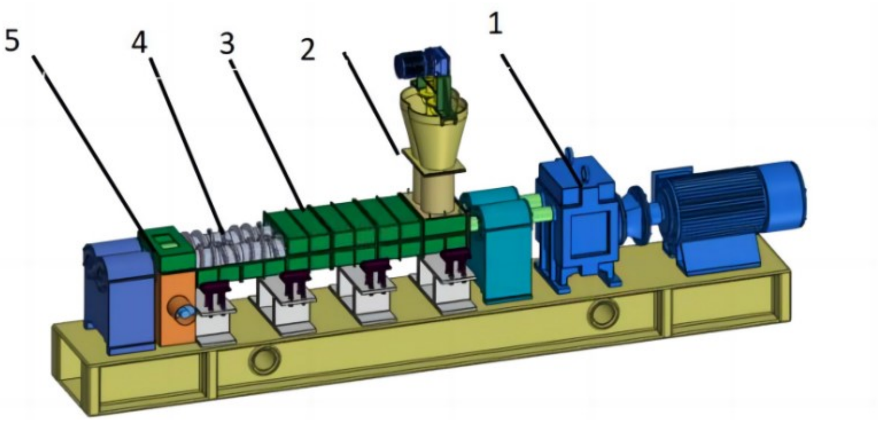

Note: 1. Electric motor; 2. Material-feeding mechanism; 3. Crushing mechanism; 4. Rolling double screws; 5. Discharge mechanism

FIGURE 1. Twin-screw rice straw crushing test device.

Test methods

To obtain statistically significant test results, the amount of straw material for each crushing test should not be less than 500 g (Chen et al., 2021). Before testing, the samples were weighed and sieved. After the test, the collected particles were weighed again to calculate the mass of particles lost during the test. The test results were available when the loss was less than 1% of the initial mass (Smith, 2016). The probabilities of particle crushing and t_{10} can be determined using the sieving method.

Crushing characteristic indexes

To study the crushing characteristics of the particles, the crushing process was quantitatively analyzed using the crushing probability (P) and particle-size distribution of the crushed products (Kruszelnicka et al., 2022). The crushing probability represents the likelihood of particle fragmentation in a crushing test and can be calculated using the following equation:

$$P = \frac{m_b}{m_t} \times 100\% \tag{1}$$

In which:

m_b-the mass of the crushed particles in the crushing test, g;

m_t- the total mass of the particle sample in the crushing test, g.

t_{10} represents the particle-size distribution of the crushed product; it indicates the percentage of particle mass that is smaller than one-tenth of the feed particle size and can be calculated using the following equation:

$$t_{10} = \frac{m_{10}}{m_t} \times 100\% \tag{2}$$

In which:

m_{10}-the mass of particles in the crushing test that passed through a sieve with a size of $L/10$, g;

L-the particle size of the rice straw particles, which was 18 mm in this study, mm.

Ab-T10 crushing model

Based on the Rocky DEM software, the commonly used normal contact model for simulating the particle-crushing process is the hysteretic linear spring model, and the tangential contact model is the linear spring Coulomb limit model (Lvov & Chitalov, 2021). The Ab-T10 crushing model was used to simulate the particle-crushing process (Nicolas, 2017). In the crushing model, the crushing of particles can be predicted based on the crushing specific energy of the particles when they come into contact with the twin screws (Ma et al., 2017). When the crushing specific energy exceeds the minimum crushing energy ($E_{\min}$) of the particle, then the particle undergoes fragmentation (Liu et al., 2016). The minimum crushing energy of a particle is related to the particle size and is calculated as follows:

$$E_{min} = E_{ref} L_{ref} / L \tag{3}$$

In which:

E_{ref}-the reference values for minimum crushing specific energy;

L_{ref}-the particle reference size, mm.

The accumulated contact specific energy (E_{cum}) is particularly important for considering the crushing of particle caused by continuous collisions (Tan et al., 2016). During the particle force process, the instantaneous contact specific energy of the particle at time t is $E_c(t)$. When $E_c(t)$ exceeds E_{min} and $E_c(t)$ exceeds E_{cummax}, then E_{cum} is expressed as follows:

$$E_{cum}(t) = E_{cum}(t - \Delta t) + E_c(t) - \max\left(E_c(t - \Delta t), E_{cummax}\right) \tag{4}$$

In which:

$E_c(t\text{-}\Delta t)$-the instantaneous contact specific energy at time t from the previous moment, J/kg;

E_{cummax}-the maximum value of accumulated contact specific energy during the particle loading process, J/kg.

During the particle-unloading process, when $E_c(t)$ decreases below E_{min}, E_{cummax} becomes 0. If the particle continues to be subjected to a force, a new loading cycle begins, and E_{cum} will accumulate again. In a single-particle-crushing test, the equation for the cumulative crushing specific energy (E_{cum}) is as follows:

$$E_{cum} = \frac{1}{2} v^2 \tag{5}$$

In which:

v-the velocity of rice straw particles in contact with twin screws.

In the Ab-T10 crushing model, the particle-crushing probability is

$$P(e_{cum}) = 1 - \exp\left(-S\left(E_{cum} - E_{min}\right) L / L_{ref}\right) \tag{6}$$

In which:

S-the coefficient of the selection function.

After particle crushing, the particle-size distribution of the sub-particles is determined by defining t_{10} as

$$t_{10} = M\left[1 - \exp\left(-S\left(E_{cum} - E_{ref}\right)\right)\right] \tag{7}$$

In which:

M-represents the maximum value that t_{10} can attain during the particle-crushing process, %.

The probability of particle breakage in the Ab-T10 crushing model is determined by ($E_{cum} - E_{min}$) and S, whereas the particle size distribution of sub-particles is determined by ($E_{cum} - E_{ref}$) and parameter M. All these parameters can be determined using single-particle-crushing tests by establishing the relationship curve between the crushing probability and $t_{10,}$ and the accumulated contact specific energy.

Construction of discrete element model for rice straw particles

The rice straw particles have different shapes, such as wedges and irregular shapes. Through tests and statistics, it was found that irregular rice straw particles account for approximately 90% of the total. Therefore, in this study, a discrete element model was established using irregular rice straw particles with moisture contents of 50%, 55%, 60%, 65%, and 70%, obtained from tests using a twin-screw pulper. The geometric structures of rice straw particles vary, and generally, three mutually perpendicular axial dimensions, namely length (L), width (W), and thickness (T), are used to represent the shape and size of the particles, as shown in Figure 2. Randomly samples 3 kg of rice straw material from 2 t of straw material fermented for 7–10 days, and three-dimensional scanning technology was used to obtain the dimensions in three axes and volume information of the rice straw particles. The length (L) was 18.00±4.50 mm, width (W) was 5.50±1.50 mm, the thickness (T) was 1.5±0.75 mm, and the volume (V) was 148.5±5.06 mm^3. One rice straw particle with dimensions and volume close to the mean values was selected (L = 14.00 mm, W = 5.00 mm, T = 2.4 mm, V = 168 mm^3) as the modeling benchmark. The three-dimensional laser scanning model of the selected rice straw particle was imported into three-dimensional software (Ansys Space-Claim), and the model was constructed using the slicing method. A cutting plane was established at the centroid of the rice straw particles, and the cutting planes were equally spaced in the positive and negative directions along the z-axis. The method of modeling rice straw particles was based on the thickness of the rice straw particles and the three-dimensional axis calibration method (McCrory et al., 201*3*). The spacing between adjacent cutting planes was set to 0.10, 0.15, 0.20, 0.25, 0.30, 0.35, 0.40, and 0.45 mm to investigate the effect of spacing on the accuracy of the model construction, and the best rice straw particle model was selected based on the results.

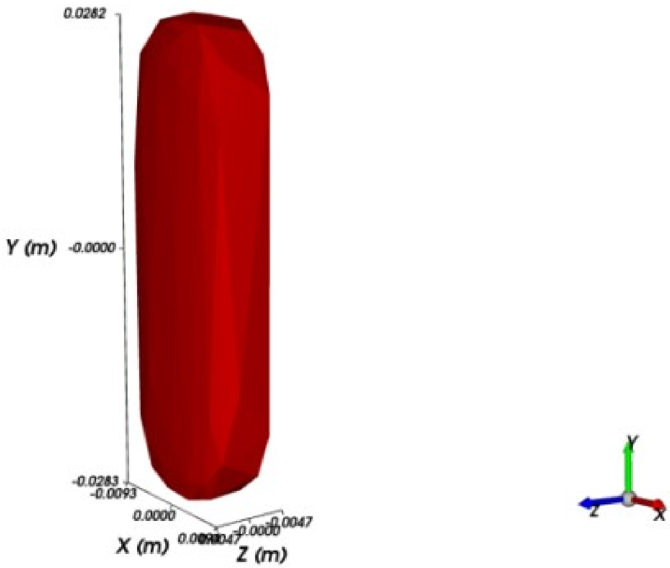

FIGURE 2. 3D scan model of rice straw material and three-axes schematic diagram.

Table 1 shows a comparison between the rice straw particle model and the actual rice straw particle size, relative error in volume, and number of faces in the particle model. From Table 1, it can be observed that the spacing between the cutting planes affects the relative error of the dimensions in three axes and volume of the model, as well as the number of faces in the model. The relative error was the highest when the spacing was set to 0.35 mm. This is because, under this spacing condition, the cutting planes cannot capture the cross-sectional profile of the edge structure of the rice straw particle, resulting in a large relative error in thickness and volume compared with the real particle model. When the spacing was set below 0.2 mm, the relative error of the dimensions in three axes and volume of the particle model compared with the real rice straw particle model was small and stable. Table 1 also shows that the number of faces in the particle model increased as the spacing between the cutting planes decreased. In discrete element simulations, when the number of particles is the same, the simulation efficiency decreases as the number of faces in each particle increases. Therefore, in this study, a cutting plane spacing of 0.2 mm was ultimately selected for modeling the rice straw particle, which ensured a small number of faces in the model, resulting in higher computational efficiency while maintaining a small relative error. The relative errors between the rice straw particle model and the actual rice straw particle in terms of the dimensions in three axes and volume were 4.5% and 0.5%, respectively, both of which were below 5%. This indicates that the constructed discrete element model has high accuracy.

TABLE 1. Comparison of the relative errors of rice straw particle model and number of constituent surfaces.

	Cutting plane spacing/mm							
	0.1	0.15	0.2	0.25	0.3	0.35	0.4	0.45
Relative error of the dimensions in three axes /%	3	5	4.5	8	2.5	9	7	5
Relative error of the volume/%	1	0	0.5	5	3	15	5	3
Number of surfaces in the particle model	17	11	6	5.5	5	2.5	3	2.5

When the rice straw particle model was imported into Rocky DEM software for crushing simulation tests, the material properties and contact parameter settings had a significant impact on the accuracy of the simulation. The bulk density of the rice straw particles was set based on a measured value (Hu et al., 2021) with a Young's modulus of 6.87 MPa and a Poisson's ratio of 0.40, as listed in Table 2.

TABLE 2. Contact parameters of rice straw particle model.

Moisture content of rice particles/%	Parameters	Rice grains-rice grains	Rice grains-twin screw
50	Static friction coefficient	0.44	0.36
	Dynamic friction coefficient	0.02	0.20
	Coefficient of restitution	0.20	0.30
	Tangential stiffness ratio	1.00	1.00
55	Static friction coefficient	0.43	0.35
	Dynamic friction coefficient	0.02	0.18
	Coefficient of restitution	0.20	0.30
	Tangential stiffness ratio	1.00	1.00
60	Static friction coefficient	0.42	0.34
	Dynamic friction coefficient	0.02	0.17
	Coefficient of restitution	0.20	0.30
	Tangential stiffness ratio	1.00	1.00
65	Static friction coefficient	0.41	0.33
	Dynamic friction coefficient	0.01	0.16
	Coefficient of restitution	0.20	0.30
	Tangential stiffness ratio	1.00	1.00
70	Static friction coefficient	0.40	0.31
	Dynamic friction coefficient	0.01	0.15
	Coefficient of restitution	0.20	0.30
	Tangential stiffness ratio	1.00	1.00

RESULTS AND DISCUSSION

Probability distribution of fragmentation and parameter calibration

It can be observed from Figure 3 that the crushing probability of rice straw particles with different moisture contents varies, and the crushing probability of rice straw particles increases with the increase in accumulated contact specific energy. When the accumulated contact specific energy is the same, the lower the moisture content of the rice straw particles, the higher the crushing probability. Sun et al. (2009) optimized the cold-pressing process of rice straw particles and concluded that drying the rice straw particles resulted in thermal stress cracks, leading to a decrease in their crushing strength. This conclusion provides a reasonable explanation for the result.

The crushing probability results of the particle-crushing tests were fitted according to [eq. (6)], and all the adjusted coefficients of determination of the fitting equation were higher than 0.995 (Figure 3). The parameters of the fitting equation were determined, which completed the calibration of parameters S and E_{ref} in the Ab-T10 crushing model, and the results (Table 3) were used for crushing simulation tests of rice straw particle.

In this study, the critical speed of the test was determined at a screw speed corresponding to a crushing probability greater than 85%. Combining the fitting equation of the crushing probability of each rice straw particle sample with different moisture contents and [eq. (5)], the critical rotation speeds of each rice straw particle sample (from low to high moisture content) were obtained as 100, 110, 120, 130, and 140 rpm, indicating that the critical crushing velocity of rice straw particles increases with the increase in moisture content. In other words, the higher the moisture content of the straw, the more difficult it is to shred. Wan (2021) studied the effect of moisture content on the crushing rate of corn straw and found that the crushing rate of straw decreased as the moisture content increased from 62.52% to 76.12%, which is similar to the conclusions obtained in this study. Wang et al. (2012) found that as an important indicator of the mechanical properties of corn stalks, the elastic modulus decreases with an increase in stalk moisture content, leading to an increase in its elasticity and cohesion. This explains why high-moisture corn stalks are more difficult to crush, resulting in a decrease in the straw breakage rate.

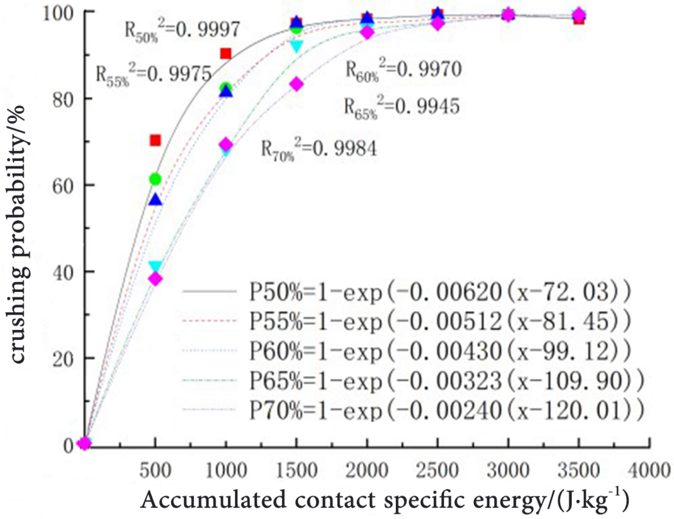

FIGURE 3. Crushing probability of rice straw particles with different moisture contents.

TABLE 3. Calibration value of *S* and *M* in Ab-T10 crushing model parameters.

Moisture content of rice straw/%	50	55	60	65	70
E_{ref}/(J·kg^{-1})	0.0062	0.00512	0.0043	0.00323	0.0024
E_{ref}/(J·kg^{-1})	72.03	81.45	99.12	109.90	120.01
M/%	12.14	11.03	9.26	7.64	4.17

t_{10} of rice straw particles and parameter calibration of Ab-T10 crushing model

It can be observed from Figure 4 that t_{10} of the rice straw particles increases with an increase in the accumulated contact specific energy. In the crushing process of actual rice straw particle, it is feasible to increase the screw speed appropriately to improve the degree of crushing of the particles, thus enhancing the crushing efficiency. It can also be noted from the figure that t_{10} of rice straw particles varies with different moisture contents. At the same accumulated contact specific energy, rice straw particles with a lower moisture content have higher t_{10} values.

Lvov & Chitalov (2021) found that the higher the plasticity of particles, the smaller and more numerous the particle size after crushing. Rice straw particles are viscoelastic in nature; with a decrease in moisture content, the intermolecular bonding forces between cellulose and hemicellulose in the rice straw particles weaken, and their brittleness increases. Therefore, smaller rice straw particles are generated after crushing, resulting in an increase in the number of rice particles, that is, an increase in the value of t_{10}.

The t_{10} results from the particle-crushing tests were fitted according to [eq. (7)], and the trend of the fitted curve was observed to be similar to the actual distribution pattern. The adjusted coefficient of determination for the fitting equation was estimated to be greater than 0.906 (Figure 4), indicating a good fit. The parameters in the fitting equation, which represent the parameter *M* in the Ab-T10 crushing model, were determined, and the results are listed in Table 3. These parameters were used to crush the rice straw particles in the simulation tests.

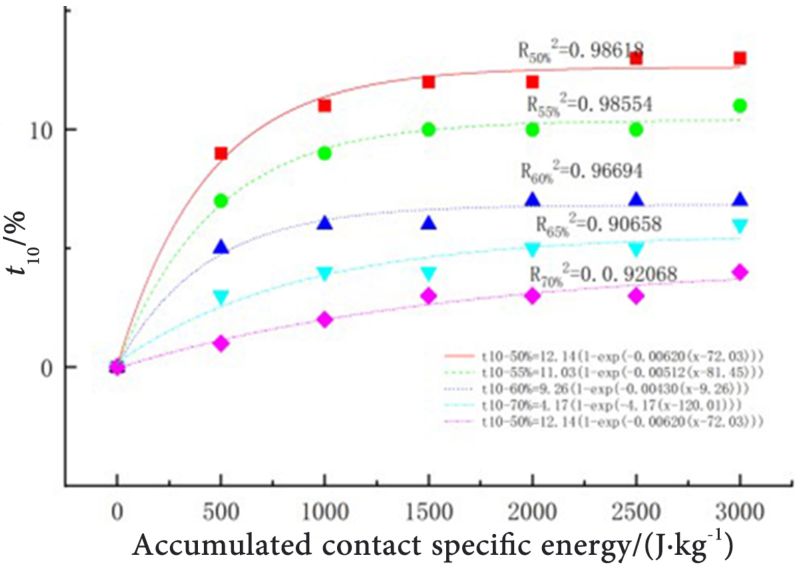

FIGURE 4. t_{10} change curve of rice straw particles with different moisture contents.

VERIFICATION TEST

The parameter calibration results of the Ab-T10 crushing model and the rice straw particle discrete element model established based on the slice method were applied to the Rocky DEM software. The crushing process of rice straw particle was simulated under actual working conditions, and the particle-size distribution law was obtained. The accuracy of the rice straw particle modeling and parameter calibration was verified by comparing the simulation results with the test data.

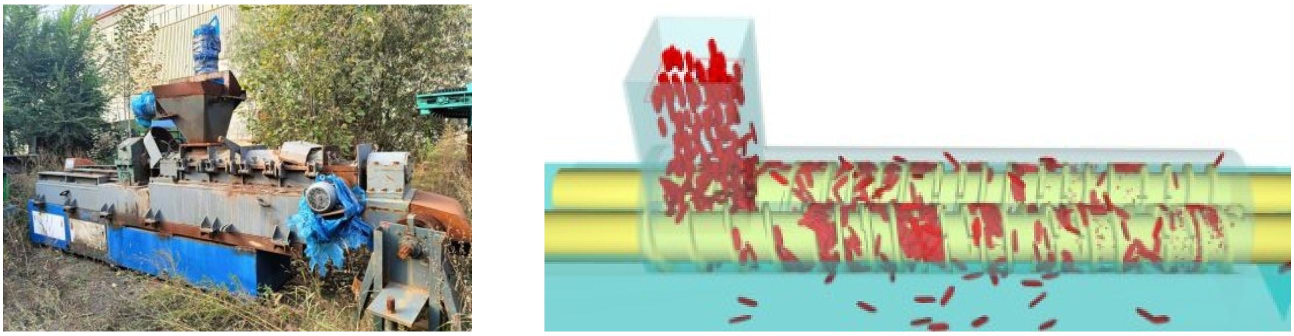

(*a*) Prototype (*b*) Simulation model

FIGURE 5. Twin-screw crusher prototype and simulation model.

The twin-screw crusher (Figure 5(a)) and simulation model (Figure 5(b)) were set with a crushing chamber width of 360 mm and a screw diameter of 180 mm. The screw speed was set to the critical crushing speed corresponding to each horizontal moisture content level, and the contact parameters corresponding to each horizontal moisture content level were used.

The minimum fitting parameter R^2 between the simulated and measured values was calculated as 0.9654 (Figure 6). According to Wang et al. (2024), Liu et al. (2024), and Dev et al. (2024), if R^2 is greater than 0.92, prediction results are accurate and credible. Hence, the calibrated model parameters and the particle model of rice straw compaction and crushing are accurate.

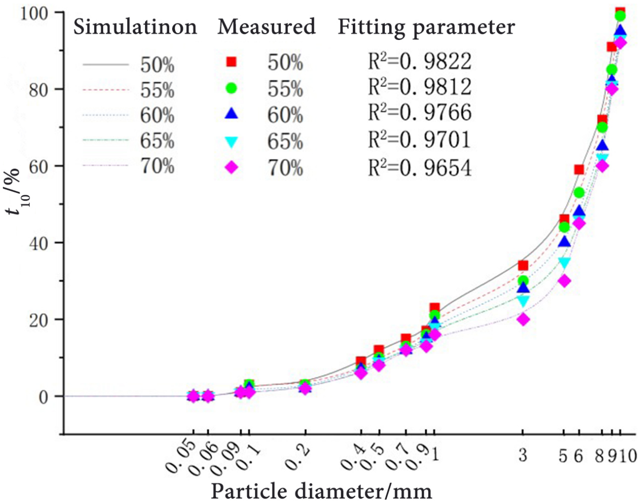

FIGURE 6. Comparison of t_{10} between simulated and measured values.

Researchers have calibrated crop parameters, providing a theoretical design basis for machinery used in the cultivation, planting, management, and harvesting of related crops (Dos Santos et al., 2017; Du & Liu, 2023; Ren et al., 2023; Shi et al., 2024b). They used a research method that combined discrete element simulation analysis with actual experiments to calibrate crop parameters and establish prediction models, which is very similar to the research method used in this study. This indicates that the research method proposed in this study is feasible and that the results are reliable.

CONCLUSIONS

The findings of this study confirm that the proposed rice straw particle modeling method can be used to establish discrete element particle models for complex agricultural materials. The results also indicate that the Ab-T10 crushing model parameter calibrated in this study has a certain degree of accuracy and can simulate and predict the fragmentation of rice straw. This study provides a reference for the analysis of crushing in subsequent rice straw pulping. This study also provides new insights for studying the crushing characteristics of other objects.

ACKNOWLEDGMENTS

We would like to express our gratitude to Dezhi Ren from Shenyang Agricultural University in Liaoning Province for the assistance provided in the sample preparation process and mass spectrometry. In addition, we would like to thank the reviewers who helped to improve the paper.

FUNDING

This research was funded by the Biological Carbonization Technology and Supporting Services Project of the Ministry of Agriculture and Rural Affairs (01101921001), Guiding Project of the Basic Research Program of Yancheng City (YCBK202213), 2022 Salt City Basic Research Program Guided Project (YCBK202239), and Shenyang Agricultural University, China.

REFERENCES

Bi SS, Yuan C, Liu C, Cheng J, Wang W, Cai YR (2021) A survey of Low-Cost 3D laser scanning technology. Applied Sciences 11(9): 3938. https://doi.org/10.3390/app11093938

Camalan M (2020) Simulating probabilistic sampling on particle populations to assess the threshold sample sizes for particle size distributions. Particulate Science and Technology 39(4): 511–520. https://doi.org/10.1080/02726351.2020.1790066

Chen GB, Wang QJ, Li WY, He J, Li HW, Yv CC (2021) Design and test of double roller differential speed crushing fertilizer device for block organic fertilizer. Transactions of the Chinese Society for Agricultural Machinery 52(12):65-76. https://doi.org/10.6041/j.issn.1000-1298.2021.12.007

Chen WF, Meng J, Han XR, Lan Y, Zhang WM (2019) Past, present, and future of biochar. Biochar 1(1): 75–87. https://doi.org/10.1007/s42773-019-00008-3

Dev A, Kumar, R, Kumar A (2024) New correlations for photovoltaic panel's efficiency and surface temperature with different operating parameters. Engenharia Agricola 46(1): 4107-4122. https://doi.org/10.1080/15567036.2024.2327596

Dos Santos MG, De Faria RT, Palaretti LF, Dantas GD, Dalri AB, Lopes AD (2017) Calibration and testing of CS-Cropgro model for common beans. Engenharia Agricola 36(6): 1239-1249. https://doi.org/10.1590/1809-4430-Eng.Agric.v36n6p1239-1249/2016

Du X, Liu CL (2023) Prediction of DEM parameters of coated fertilizer particles based on GA-BP neural network. Engenharia Agricola 43(S1): e20210099. https://doi.org/10.1590/1809-4430-Eng.Agric.v43nepe20210099/2023

Goda I, Girardot J (2021) Numerical modeling and analysis of the ballistic impact response of ceramic/composite targets and the influence of cohesive material parameters. International Journal of Damage Mechanics 30(7):1079-1122. https://doi.org/10.1177/1056789521992107

Habert G, Miller SA, John VM, Provis JL, Favier A, Horvath A, Scrivener K (2020) Environmental impacts and decarbonization strategies in the cement and concrete industries. Nature Reviews Earth & Environment 1(11): 559–573. https://doi.org/10.1038/s43017-020-0093-3

Hu J, Deng J, Deng Y, Chen T, Wang G, Sun Z, Guo H (2021) Contact parameter analysis and calibration in discrete element simulation of rice straw. International Journal of Agricultural and Biological Engineering 14(3): 72–81. https://doi.org/10.25165/j.ijabe.20211404.6435

Kruszelnicka W, Diviš J, Hlosta J, Gierz Ł, Žurovec D (2022) Calibration of selected bulk biomaterials parameters for DEM simulation of comminution process. Case study: Corn and rice grains. Advances in Science and Technology Research Journal 16(5): 64–77. https://doi.org/10.12913/22998624/152990

Lai YM, Li JB, Li QZ (2012) Study on damage statistical constitutive model and stochastic simulation for warm ice-rich frozen silt. Cold Regions Science and Technology 71: 102–110. https://doi.org/10.1016/j.coldregions.2011.11.001

Liu BY, Chen ZY, Li B, Wu SF, Feng H, Gao XD, Siddique KHM (2024) Modeling of driving factors and headcut rates of ephemeral gullies in the loess plateau of China using high-resolution remote sensing images. International Journal of Digital Earth 17(1): 2369632. https://doi.org/10.1080/17538947.2024.2369632

Liu LF, Thornton C, Shaw SJ, Tadjouddine EM (2016) Discrete element modelling of agglomerate impact using autoadhesive elastic-plastic particles. Powder Technology 297: 81–88. https://doi.org/10.1016/j.powtec.2016.04.009

Lvov VV, Chitalov L (2021) Semi-Autogenous Wet Grinding Modeling with CFD-DEM. Minerals 11(5): 485. https://doi.org/10.3390/min11050485

Ma G, Zhou W, Regueiro RA, Wang Q, Chang XL (2017) Modeling the fragmentation of rock grains using computed tomography and combined FDEM. Powder Technology 308: 388–397. https://doi.org/10.1016/j.powtec.2016.11.046

McCrory CCL, Jung S, Peters, JC, Jaramillo TF (2013) Benchmarking heterogeneous electrocatalysts for the oxygen evolution reaction. Journal of the American Chemical Society 135(45): 16977–16987. https://doi.org/10.1021/ja407115p

Nicolas M (2017) A comprehensive study on the behavior of a rigid block on an oscillating ground with friction, elastic and viscous forces. International Journal of Non-Linear Mechanics 93: 21–29. https://doi.org/10.1016/j.ijnonlinmec.2017.04.017

Ren D, Zhang L, Gong Y, Meng J, He T (2023) Calibration and testing of discrete element model parameters for biochar-based fertilizer. Journal of Shenyang Agricultural University 54(4): 447-455. https://doi.org/10.3969/j.issn.1000-1700.2023.04.008

Shahrubudin N, Lee TC, Ramlan R (2019) An overview on 3D printing technology: technological, materials, and applications. Procedia Manufacturing 35: 1286–1296. https://doi.org/10.1016/j.promfg.2019.06.089

Shi JP, Shan ZD, Yang HQ (2024a) Research on the macro- and meso-mechanical properties of frozen sand mold based on Hertz-Mindlin with Bonding model. Particuology 88: 176-91. https://doi.org/10.1016/j.partic.2023.08.019

Shi ZL, Wang MJ, Zhang XJ, Cheng JP, Lu DM (2024b) Calibration and optimization of discrete element parameters for coated cotton seed. Engenharia Agricola 44: e20230085. https://doi.org/10.1590/1809-4430-Eng.Agric.v44e20230085/2024

Singh S, Ramakrishna S, Singh R (2017) Material issues in additive manufacturing: A review. Journal of Manufacturing Processes 25: 185–200. https://doi.org/10.1016/j.jmapro.2016.11.006

Smith DR (2016) Preharvest food safety challenges in beef and dairy production. Microbiology Spectrum 4(4). https://doi.org/10.1128/microbiolspec.pfs-0008-2015

Sun Q, Bai HC, Gu SY, Zhang CM, Gao W, Yi WM (2009) Optimization of cold press molding process conditions for rice straw pellet. Journal of Agricultural Machinery 40(8): 100-4.

Tan YZ, Hu MZ, Li DQ (2016) Effects of agglomerate size on California bearing ratio of lime treated lateritic soils. International Journal of Sustainable Built Environment 5(1): 168–175. https://doi.org/10.1016/j.ijsbe.2016.03.002

Tian D, Guo SG, Wang LY (2023) Design and 3D flow analysis Based on ANSYS/CFX stepwise acceleration twin screw. Food & Machinery 39(6): 99-104. https://doi.org/10.13652/j.spjx.1003.5788.2022.80983

Wan YB (2021) Performance experiment and optimization on stalk vertical chopping device of maize combine harvester. Northeast Agricultural University. https://doi.org/10.27010/d.cnki.gdbnu.2020.000932

Wang CF, Mao M, Pan JM, Yu Y, Teng B (2012) Study of Sampling Conditions on the Elastic Modulus of Corn Straw. Agricultural Engineering 2(1): 48-53

Wang JM (2022) The application of plant fiber slurry in the slurry mold. Chinese packaging 42(12): 23-26.

Wang ZY, Ling JM, Du H, Zhang JK, Li X (2024) Performance prediction for network-level flexible pavements using an optimised ANN approach. International Journal of Pavement Engineering 25(1): 2329231. https://doi.org/10.1080/10298436.2024.2329231

Wu H, Lu SY, Chen D (2024) Concrete 3D mesoscale model-based study on dynamic shear behavior of FRP-concrete bonding interface [OL]. Engineering Mechanics. https://doi.org/10.6052/j.issn.1000-4750.2023.08.0567

Yu X, Zheng H, Sun L, Shan YL (2020) An emissions accounting framework for industrial parks in China. Journal of Cleaner Production 244: 118712. https://doi.org/10.1016/j.jclepro.2019.118712

Zhang M, Feng B, Wang XK, Yin MF, Zhang X, Sun GH, Ma JS, Cheng DB, Hou LL (2023) Research progress in preparation and application of natural fiber reinforced thermoplastic composites. Engineering Plastics Application 51(10): 179-185. https://doi.org/10.3969/j.issn.1001-3539.2023.10.027

Zhang RF, Zhou JL, Liu H, Shi S, Wei GJ, He TF (2022) Determination of interspecific contact parameters of corn and simulation calibration of discrete element. Transactions of the Chinese Society for Agricultural Machinery 53(S1):69-77. https://doi.org/10.6041/j.issn.1000-1298.2022.S1.008